A Stacked-Photovoltaic-Cell Energy Harvester with >81% Indoor Light Harvesting Efficiency for Millimeter-Scale Energy-Autonomous Sensor Nodes

Yuyang Li[1], Eunseong Moon[2], Jamie Phillips[3], and Inhee Lee[1]
[1]University of Pittsburgh, Pittsburgh, USA; [2]University of Michigan, Ann Arbor, USA; [3]University of Delaware, Newark, USA
yul230@pitt.edu, esmoon@umich.edu, jphilli@udel.edu, inhee.lee@pitt.edu

ESSCIRC 2021 - IEEE 47th European Solid State Circuits Conference (ESSCIRC) | 978-1-6654-3751-6/21/$31.00 ©2021 IEEE | DOI: 10.1109/ESSCIRC53450.2021.9567847

***Abstract*— We propose a light energy harvester that achieves harvesting efficiency of 82 – 98% at indoor light levels (70lx – 1klx) and powers a millimeter-scale system even at 40lx. It improves the efficiency by connecting stacked photovoltaic (PV) cells directly to a battery without diode voltage drop and implementing essential battery protection functions, such as battery discharging/overcharging protection and initial-battery-charging delay, in 334pA. The proposed circuit monitors open-circuit voltage of the stacked PV cells indirectly with a tiny auxiliary cell (only 0.16% area penalty) for battery discharging protection without interrupting energy harvesting. It also delays the initial battery charging by 3.9 hours, long enough to avoid accidental battery charging during a system assembly process.**

Keywords—energy harvesting, battery protection, miniature system

I. Introduction

Millimeter-scale systems recently became attractive monitoring tools for biomedical, ecological, and IoT applications [1]. The advanced system, with a small battery, is fully encapsulated for physical protection, and it employs an energy harvester to extend its lifetime. The full encapsulation does not allow any external connection and thus impose strict conditions on the energy harvester. First, it must maintain high harvesting efficiency at weak harvesting energy environment and nominal battery operating voltage. This is critical since external power cannot be connected for battery charging, and the small energy harvesting device (e.g., photovoltaic (PV) cells) can provide limited energy due to the system-size constraint. Second, it must consume low quiescent current while protecting a battery from being 1) discharged in a low harvesting energy condition, 2) overcharged to high voltage, and 3) accidentally charged during a system assembly process [2]. Maintaining a battery uncharged before actual operation is essential since the assembly process of millimeter-scale systems requires high temperature to cure encapsulation, which can damage a charged lithium battery. Also, a system can be stored in long time without energy harvesting source (e.g., light) before actual operation so that battery capacity can be permanently reduced if a charged battery is discharged below a cut-off voltage. Thus, there is a potential risk that the battery is discharged by leakage below the voltage.

To meet these requirements, we propose an energy harvester that efficiently charges a battery, particularly at indoor light levels (<1klx) and typical lithium-battery voltage (3.6 – 4.1V), and protects its battery from battery discharging, overcharging, and accidental charging before actual operation in only 334pA at 4V. The energy harvester consists of 7.8mm^2 integrated AlGaAs PV cells, optimized for weak light levels [3] and 0.11mm^2 CMOS circuits. Six AlGaAs PV cells, connected in series electrically, provide high voltage and directly charge a ~4V battery through a PMOS switch. It enables high harvesting efficiency of 82 – 98% at 70lx – 1klx

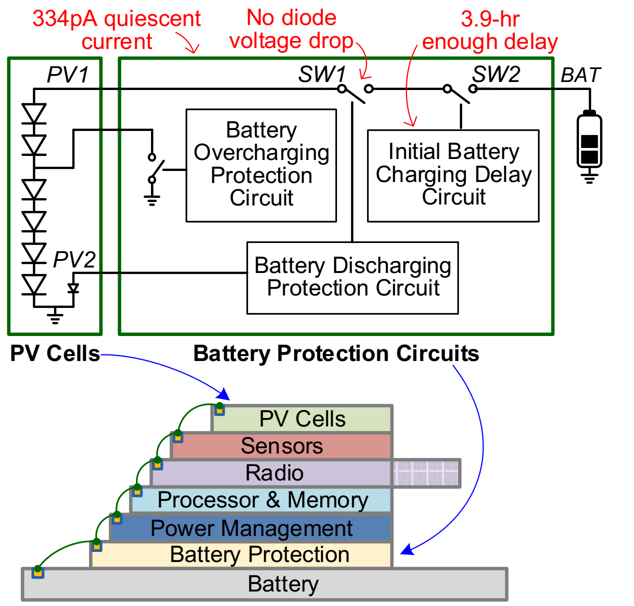

Fig. 1. Proposed energy harvester with stacked PV cells and battery protection circuits for millimeter-scale sensing systems.

by avoiding a switching loss [4] or diode voltage drop [2]. The proposed circuit monitors voltage of a small auxiliary PV cell (only 0.16% area of the total PV cells) and check if there is a risk that the main PV cells discharge the battery, without disconnecting the main cells and thus interrupting energy harvesting. Also, it delays the first battery charging by 3.9 hour reliably to not charge the battery during an assembly process. The long delay simplifies light control compared with a 1-min short delay [2], by not requiring frequent delay reset. After the delay, it continuously connects the PV cells to the battery, not imposing any delay for the following battery charging. Due to the high energy efficiency at low light levels and low power consumption, the proposed harvester can power an advanced millimeter-scale system even at 40lx without energy draw from the battery.

II. Proposed Energy Harvester

Fig. 1 describes the proposed energy harvester, which can be implemented in a millimeter-scale system [1]. It consists of PV cells, battery discharging/overcharging protection circuits, and initial-battery-charging delay circuit. The stacked six PV cells charge the battery through PMOS switches without an energy loss from diode voltage drop. Fig. 2 shows the proposed battery discharging/overcharging protection circuits. It compares divided battery voltage (*vbatdiv1*) with the voltage of the tiny auxiliary PV cell (*PV2*) to disconnect the battery switch (*SW1*) when light is not strong enough to charge the battery. It also compares another divided battery voltage (*vbatdiv2*) with reference voltage (1.2V) and pulls down the middle node of the PV cells to not overcharge the battery above ~4.2V. The circuits consume 167 – 289pA at

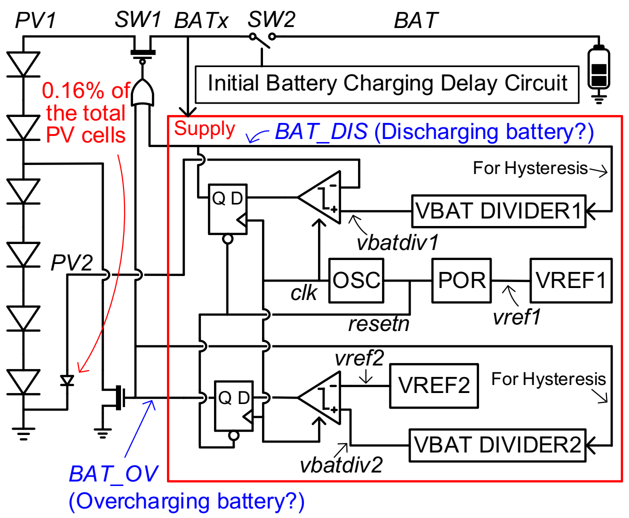

Fig. 2. Battery discharging and overcharging protection circuits.

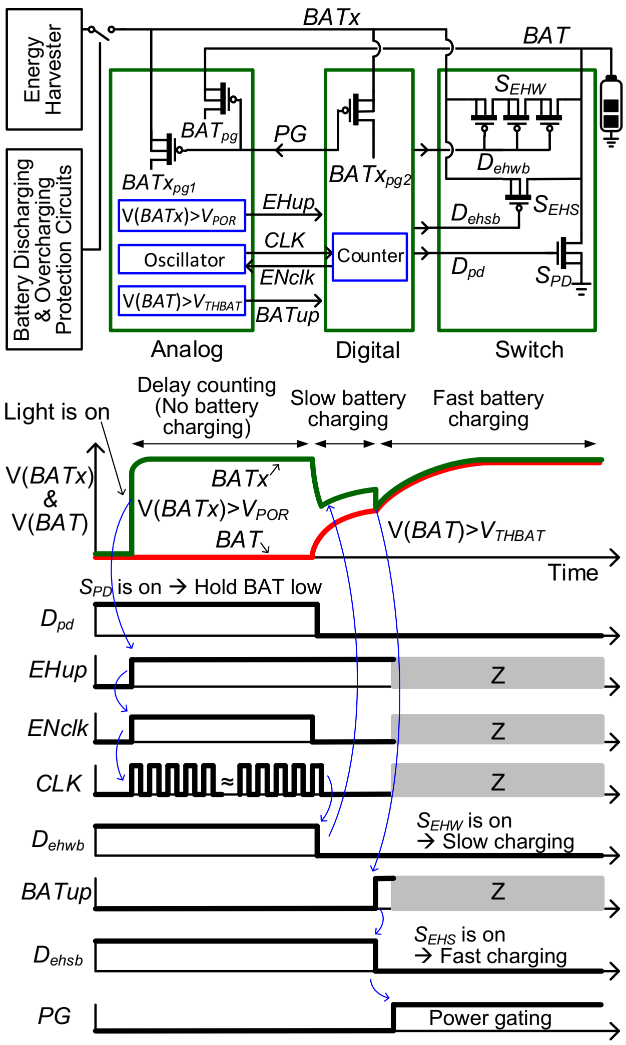

Fig. 3. Initial-battery-charging delay circuit.

3.6 – 4.1V (average from measured 8 samples) while checking the status at a frequency of ~10Hz.

Fig. 3 shows the initial-battery-charging delay circuit. Once the supply voltage (*BATx*) is higher than a threshold (3.5V), it counts reliable 597Hz pulses (*CLK*) for 3.9-hour delay while consuming 1.4µA only for the delay period. If

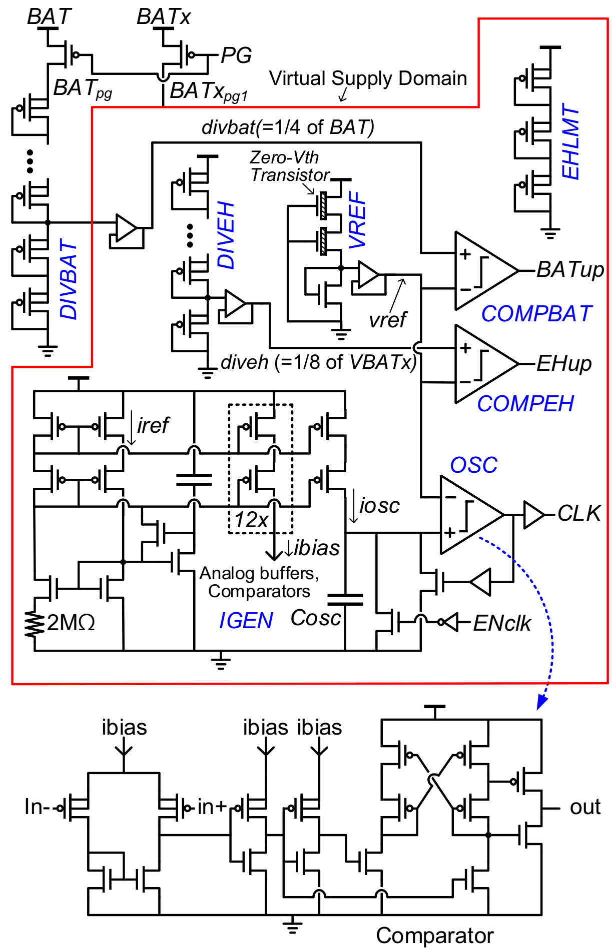

Fig. 4. Circuit diagram of the analog block of the initial-battery-charging delay circuit.

light becomes weaker during the period, the delay is reset in a short time (59µs in simulation). Otherwise, it turns on a weak switch (S_{EHW}) to start battery charging and then a strong switch (S_{EHS}) when V(*BAT*) = V_{THBAT} (1.8V). Note that the high resistance of S_{EHW} prevents circuit malfunction from low V(*BAT*) of the uncharged battery by allowing voltage drop across the switch and maintaining V(*BATx*) high enough. After the delay, it power-gates most of circuits, which significantly reduces power consumption of the circuit down to 61.7 – 90.6pA at 3.6 – 4.1V (average from measured 24 samples) and boosts battery charging.

Fig. 4 shows the circuit diagram of the analog block. It mainly detects if V(*BATx*) and V(*BAT*) reach V_{POR} and V_{THBAT}, respectively, and generates a clock signal. For the operations, the block consists of two continuous comparators (*COMPEH* and *COMPBAT*), two voltage dividers (*DIVEH* and *DIVBAT*), a voltage reference (*VREF*), a relaxation oscillator (*OSC*), and a bias current generator (*IGEN*). *COMPEH* compares *diveh* (=1/8 of V(*BATx*)) with *vref* and finds if V(*BATx*) is higher than 3.5V to set *EHup* high. *COMPBAT* compares *divbat* (=1/5 of V(*BAT*)) with *vref* and senses if V(*BAT*) is higher than 1.8V to set *BATup* high. The two comparators use the same design where current-starved inverters convert the single-ended output of an amplifier to a differential signal. It helps a level converter to shift low-voltage inputs (e.g., 1.1V) to a high-voltage output (e.g., 3.9V). *DIVEH* and *DIVBAT* consumes only 4.2nA and 1.7nA at 4V, respectively, by using diode-connected PMOS transistors connected in series instead of using resistors. *VREF* generates a reference voltage (*vref*)

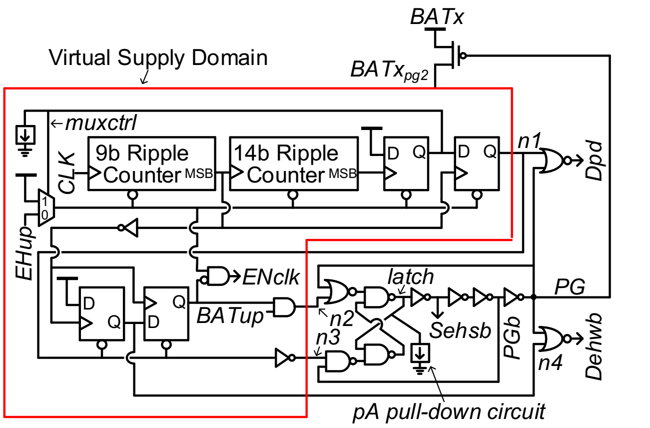

Fig. 5. Circuit diagram of the digital block of the initial-battery-charging delay circuit.

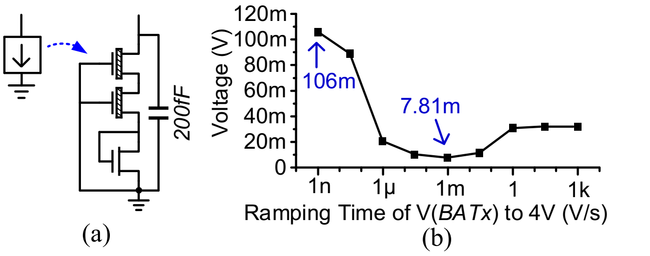

Fig. 6. Initialization of the digital block. (a) Pull-down circuit; (b) Simulated maximum voltage of *muxctrl* and *latch*.

of 361mV using a subthreshold CMOS voltage reference [5] while consuming only 2.5nA. Analog buffers are followed by *DIVEH*, *DIVBAT*, and *VREF* to protect the high-impedance nodes from switching noise. *OSC* generates a 597Hz clock signal (*CLK*) based on a relaxation oscillator that charges a metal-insulator-metal capacitor (*Cosc*) of 18pF by *iosc* of 4nA. *IGEN* employs a beta-multiplier reference with a 2MΩ resistor and creates *iref* of 20.7nA. It supplies all the bias current for the analog buffers, comparators, and an oscillator through current mirrors. The current mirror includes two stacked PMOS transistors to maintain its accuracy at high supply voltage. *EHLMT* limits V(*BATx*) using stacked, diode-connected PMOS transistors to protect circuits from too high supply voltage. *EHLMT* enables a manufacturer to use light intensity up to 35klux, which is enough for manufacturing processes for the system. Once S_{EHS} is connected, all the circuits are power-gated by a PMOS transistor with *PG* to reduce quiescent current.

Fig. 5 presents the circuit diagram of the digital block. It receives *EHup*, *BATup*, and *CLK* from the analog blocks and controls S_{EHW}, S_{EHS}, and S_{PD} and sends *PG* and *ENclk* to the analog block. As the supply voltage (V(*BATx*)) rises from ground, two pA pull-down circuits hold the control voltage of a mux (*muxctrl*) and the SR latch output (*latch*) to ground. As shown in Fig. 6 (a), the pull-down circuit consists of a pA current reference and a decoupling capacitor of 200fF, which hold the node low for slow and fast rising V(*BATx*), respectively. However, low static current of the circuit helps not to disturb original logic operations after V(*BATx*) is risen. Fig. 6 (b) shows the simulated maximum voltages of *muxctrl* and *latch* by increasing V(*BATx*) across temperatures (0-100°C) and corners with different speeds. The low voltage (0.03% of V(*BATx*)) is important since *latch* directly controls *PG* that enables most of circuits from the beginning and

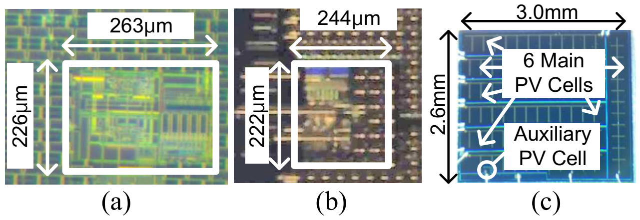

Fig. 7. Chip photographs. (a) Battery overcharging /discharging protection circuit; (b) Initial battery charging delay circuit; (c) PV cells.

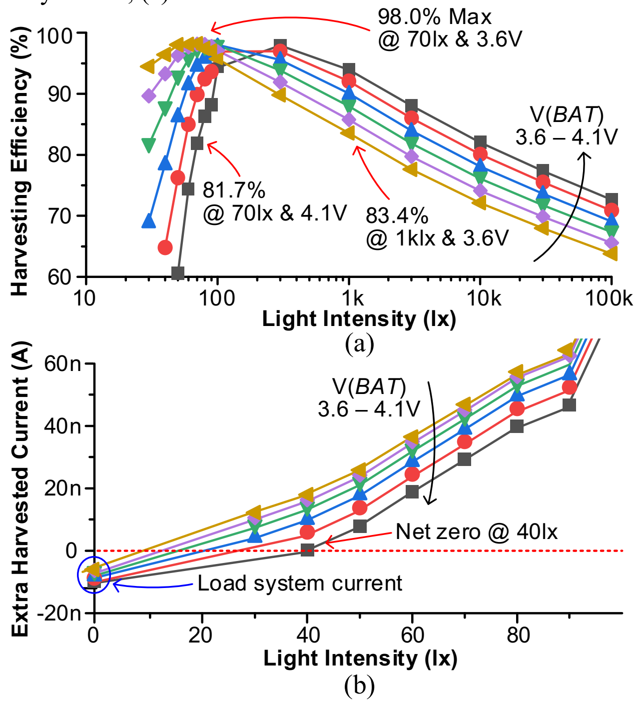

Fig. 8. Measured energy harvester. (a) Harvesting efficiency; (b) Extra harvested current while supporting a nano-watt millimeter-scale system.

muxctrl resets all the counters and flip-flops. As V(*BATx*) increases and the analog block sets *EHup* high, it sets *ENclk* high and makes *OSC* in the analog block generate a 597Hz clock (*CLK*). The 9b and 14b ripple counters count pulses of *CLK*. Once MSB of the 14b counter becomes high, logics set *PD* high, D_{ehwb} low, and *ENclk* high in sequence. Low D_{ehwb} turns on S_{EHS}, and *BAT* is charged by *BATx*. As V(*BAT*) increases and the analog block sets *BATup* high, circuits in the digital block set *latch* high, D_{ehsb} low, and *PG* high. High *PG* power-gates the entire analog block and most of the digital block. To avoid short-circuit current due to floating signals from the power-gated block, the boundary nodes (*n1*, *n2*, *n3, and n4*) are isolated by *PG* or *PGb*.

III. Measurement Results

Fabricated in a 180nm CMOS process, the proposed circuit was tested with the custom PV cells (Fig. 7). The measured harvesting efficiency is 82 – 98% for indoor light levels (70lx –1klx) (Fig. 8), including a 1.1% PV-cell area loss from the tiny auxiliary PV cell, pads for series connection, and trench isolation between cells and with quiescent current (229 – 380pA at 3.6 – 4.1V). It is higher than the previous best reported efficiency (78 – 95% [6]) at <1klx among fully integrated light harvesters. The efficient harvesting approach enables to power a millimeter-scale system, consisting of a processor, memory, a radio, sensors, and a power management

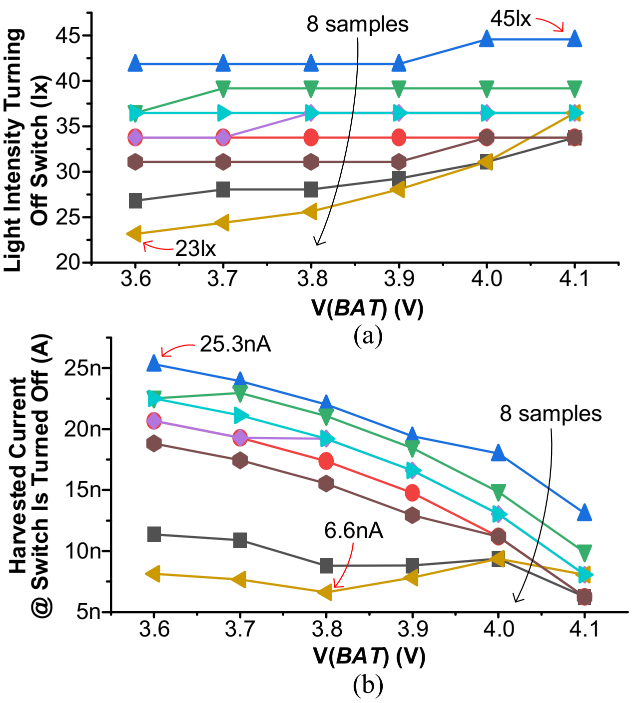

Fig. 9. Measured discharging protection. (a) Light intensity turning off *SW1*; (b) Marginal harvested current when *SW1* is turned off.

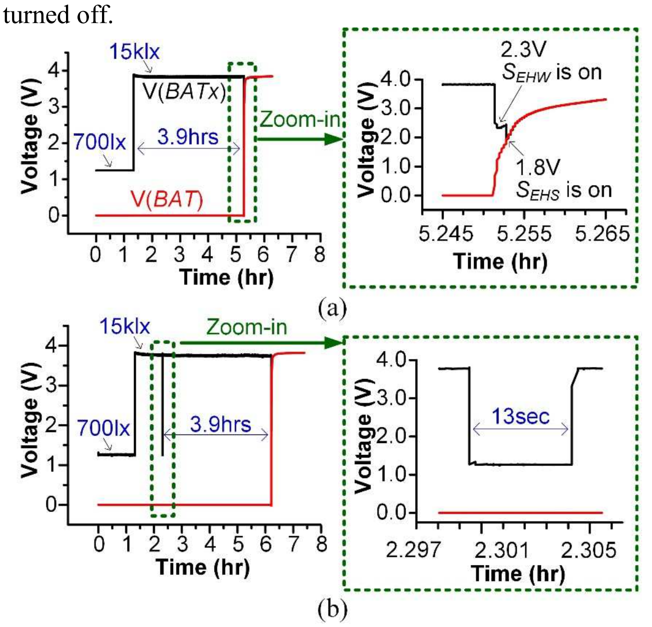

Fig. 10. Measured initial-battery-charging delay circuit. (a) Continuous light; (b) Delay-reset condition with turned-off light in the middle.

unit, without drawing energy from a battery, even at 40lx (very dark condition). The measured battery discharging protection circuit (Fig. 9) disconnects *SW1* (Fig. 2) at 23 – 45lx and prevents battery energy loss with a low harvested current margin of 6.6 – 25.3nA. The measured battery overcharging protection circuit stops energy harvesting when V(*BAT*) reaches 4.12 – 4.25V (8 samples, 4.16V on average). The two protection circuits consume 225 – 343pA at 4V (8 samples, 250pA on average). The measured initial-battery-charging delay circuit obtains the average delay of 3.9 hours (σ/μ = 4.4%, line sensitivity = 2.5%/V) and the average quiescent current of 84pA at 4V (σ/μ = 21%, line sensitivity = 99%/V) from 24 samples. Fig. 10 displays its measured waveforms for a typical condition with continuous light and a

Table I. Performance summary and comparison with the state-of-the-art fully integrated light energy harvesters.

	This Work	VLSI'18 [2]	JSSC'14 [4]	ISSCC'15 [6]
Harvester Type	Stacked PV	Stacked PV	Charge Pump	Stacked PV
Harvest Efficiency for Indoor Light (<1klx)	82–98% (>70lx)	72–90% (>400lx)	10–43% (>70lx)	78–95% (>100lx)
Quiescent Current	334pA @4V	209pA @4V	1.7nA @5.2V	1.0nA @2V
Batt. Overcharge Protection	Yes	Yes	No	No
Batt. Discharge Protection	Yes (Switch)	Yes (Diode)	Yes (Inherent)	No
Initial Batt. Charge Protection	Yes (3.9hr)	Yes (1min)	No	No
Area (mm^2)	0.11	0.10	0.86	0.19
PV Cell Size (mm^2)	7.80	1.43	0.84	9.00

delay-reset condition with 13s turned-off light. Note that the S_{EHW} (weak switch) enables to maintain V(*BATx*) at 2.3V even with V(*BAT*) = 0V, to not lose the delay status for the typical condition. Compared with the previous works (Table I), the proposed energy harvester achieves the highest harvesting efficiency at indoor light levels (<1klx), where the efficiency is critical for miniature systems. This work and [2] include all the essential battery protection functions, but this work achieves 8 – 10% higher harvesting efficiency by a battery switch and simplifies light control during an assembly process by 234× longer initial-battery-charging delay.

IV. Conclusion

We propose a light energy harvester with stacked PV cells and low-power battery protection circuits. It achieves harvesting efficiency of 82 – 98% at indoor light levels (70lx – 1klx) and powers a millimeter-scale system even at 40lx, by avoiding diode voltage drop and implementing essential battery protection functions in only 334pA. Compared with the previous fully integrated light harvesters, it achieves the highest harvesting efficiency at indoor light levels and simplifies light control during an assembly process by 234× longer initial-battery-charging delay.

Acknowledgment

This research was supported in part by the University of Pittsburgh Center for Research Computing through the resources provided.

References

[1] D. Blaauw, *et al.*, " IoT design space challenges: Circuits and systems," in *Dig. Symp. VLSI Technology,* Jun. 2014, pp. 1-2.

[2] I. Lee, *et al.*, "A 179-lux energy-autonomous fully-encapsulated 17-mm^3 sensor node with initial charge delay circuit for battery protection," in *Proc. Symp. VLSI Circuits*, Jun. 2018, pp. 251-252.

[3] E. Moon, I. Lee, D. Blaauw, and J. D. Phillips "High-efficiency photovoltaic modules on a chip for millimeter-scale energy harvesting", *Prog Photovolt Res Appl.*, Mar., 2019, pp. 540 – 546.

[4] W. Jung, *et al.*, "A 3nW Fully Integrated Energy Harvester Based on Self-Oscillating Switched-Capacitor DC-DC Converter," in *Dig. Intl. Solid State Circ. Conf.*, Feb., 2014, pp. 398 – 400.

[5] M. Seok, G. Kim, D. Blaauw, and D. Sylvester, "A Portable 2-Transistor Picowatt TemperatureCompensated Voltage Reference Operating at 0.5 V," *J. Solid-State Circuits*, vol. 47, no. 10, pp. 2534-2545, Oct. 2012.

[6] I. Lee, *et al.*, "A >78%-efficient light harvester over 100 – to – 100klux with Reconfigurable PV-Cell Network and MPPT Circuit," in *Dig. Intl. Solid State Circ. Conf.*, Feb., 2016, pp. 370 – 372.